Journal of Thermal Analysis and Calorimetry, Vol. 55 (1999) 397-412

ACOUSTIC WAVE MASS SENSORS

Z. Ali

School of Science and Technology, University of Teesside, Middlesbrough, TS1 3BA, UK

Abstract

The application of acoustic wave microsensors for mass sensing will be reviewed with focus on the quartz crystal microbalance (QCM) and surface acoustic wave (SAW) devices. The use of QCM and SAW devices in chemical sensing as well as in the determination of solid and liquid properties will be described. In chemical sensing, it is unlikely that a single sensor with a single coating will display a selective and reversible response to a given analyte in a mixture. Alternative strategies such as the use of sensor arrays and the use of sampling devices can be used to improve performance. QCM sensors (QCMs) will oscillate under liquids; their use in under-liquid sensing will be discussed.

Keywords: acoustic wave, gas, liquid, mass, QCM, sensor

Introduction

The major types of acoustic microsensors include quartz crystal microbalance (QCM) devices, surface acoustic wave (SAW), flexural plate wave (FPW), and acoustic plate mode (APM). The common feature of these devices is that they employ piezoelectricity to generate acoustic waves; acoustic waves can, however, be generated magnetostrictively, electrostrictively and photothermally. Acoustic wave devices can be used to measure various properties of solid or fluid media in contact with their surfaces including liquid density, liquid viscosity, polymer modulus and electrical conductivity.

In sensing applications, the device is required to generate acoustic waves and methods to measure wave characteristics, such as wave velocity, frequency and/or amplitude. Interaction of the measurand directly or indirectly with the acoustic wave leads to changes in the wave characteristics and give indication of the measurand. For use of acoustic wave microsensors in chemical sensing, a chemical layer is added to the device which selectively abstracts the analyte from the medium being analysed to the device surface where it alters one or more properties of the acoustic wave. A wide range of chemically selective layers can be employed including bioreceptors, thin polymer or organic films, transition-metal complexes, electroactive materials, metal films and metal oxide films. Grate *et al.* [1, 2] have given an excellent description of the different device

1418–2874/99/ $ 5.00

Akadémiai Kiadó, Budapest
Kluwer Academic Publishers, Dordrecht

types. The two major types of piezoelectric devices are the QCM and SAW. The QCM devices, which are also known as bulk wave devices or thickness shear mode (TSM), operate by transmitting a bulk wave from one crystal face to the other. TSM is a more generic term since it does not presuppose the substrate material. Surface acoustic wave (SAW) devices operate by transmitting waves along a single crystal face from one location to another.

Quartz crystal microbalance

Piezoelectricity was discovered in 1880 by the Curie brothers as a phenomenon where electric dipoles are generated in anistropic natural crystals subjected to mechanical stress [3]. The converse effect was predicted by Lippmann [4] and is the basis of the QCM. Piezoelectricity occurs in the 21 classes of crystals that do not possess a centre of symmetry. Alpha quartz is a widely-used piezoelectric material owing to its water insolubility and resistance to temperature, up to 573°C, with no loss of piezoelectric properties. The application of electric fields across the boundaries of a piezoelectric crystal results in the creation of particle displacement and strains. The magnitude of transduction between electrical and mechanical forces is dependent on the values of piezoelectric coupling constants. The direction of particle displacement and velocity of an acoustic wave can be varied by using piezoelectric crystals of different symmetries and by generating acoustic wave at different orientations with respect to the crystallographic axes. The QCMs are AT-cut since a zero temperature coefficient is observed at room temperature. Thickness is the frequency determining parameter in these devices.

The harmonic motion of a quartz crystal is analogous to that of a mass on a spring, a pendulum, or a vibrating string. The shear motion of the quartz crystal occurs between the limits $-x_{max}<x<+x_{max}$ with x_{max} being dependent upon the applied voltage of the quartz crystal. Quartz resonators have the ability to oscillate with minimal loss of energy. The ratio of peak energy stored to energy lost per cycle is known as the Q-factor and for quartz crystals can be in excess of 100 000. The mechanical model of a QCM is shown in Fig. 1 and the corresponding electrical equivalent is shown in Fig. 2. L is the inertial component related to the displaced mass (M), C_1 is the compliance (defined as the ability of an object to yield elastically when a force is applied) of the quartz crystal and represents the energy

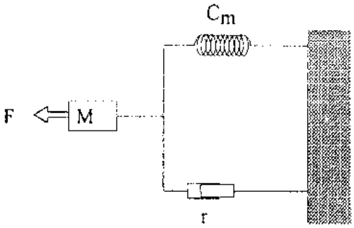

Fig. 1 Mechanical model of QCM

stored during oscillation (C_m), and R_1 is the energy dissipation during oscillation due to internal friction, losses due to the QCM mounting and acoustical losses to the surroundings (r). The electrical equivalent circuit has an additional capacitance (C_o) in parallel to the series arm and represents the static capacitance of the quartz resonator with the electrodes. The series branch is referred to as the motional branch since it describes the electromechanical behaviour of the QCM [5].

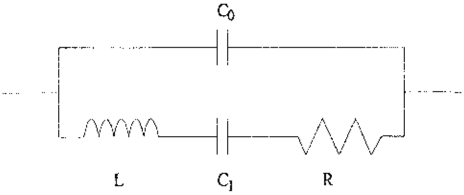

Fig. 2 Electrical equivalent of QCM

The oscillating properties of the QCM have been described by Buttry and Ward [5] in terms of a simple LCR tank circuit shown in Fig. 3. When the switch is fully open the capacitor is fully charged, but when the switch is closed current passes through the inductor and a magnetic field is developed. When the capacitor becomes fully discharged the current goes to zero and the magnetic field begins to decrease, inducing an Emf in the inductor in a direction opposite to the intial current. The current flows until the magnetic field has disappeared and the capacitor becomes fully charged, albeit with reverse polarity. The process can be repeated indefinitely if $R=0$. If $R>0$ then the oscillation will be dampened over time. The quartz crystal at displacement $x=\pm x_{max}$ is equivalent to the capacitor being fully charged. At this point the potential energy is at a maximum and the kinetic energy is at a minimum. The condition $x=0$ is equivalent to the LCR tank circuit with the capacitor fully discharged, maximum magnetic field around the inductor and maximum current, representing maximum kinetic energy.

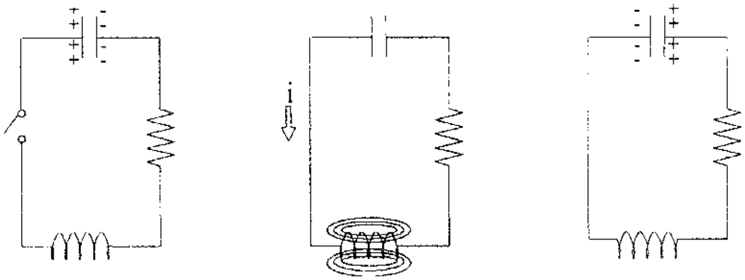

Fig. 3 LCR tank circuit model of QCM oscillation

A QCM is constructed by applying metal electrodes to the surfaces of a thin piezoelectric plate (Fig. 4). Acoustic waves are generated by applying an oscillating electrical field between the plates. The acoustic displacement induced will depend upon the piezoelectric coupling and elastic stiffness constants of the material. Only acoustic waves satisfying the boundary conditions of the resonator surface will propagate efficiently across the device [6]. Such waves can be modelled as standing sinusoidal waves which have nodes of displacement at the resonator surfaces. Waves that will resonate (transmit efficiently) follow the relation:

$$\frac{\omega}{V}=\frac{2\pi}{L}=\frac{N\pi}{D} \quad N=1, 3, 5,\ldots \tag{1}$$

where ω is the angular frequency of the acoustic wave, V is wave velocity, L is the acoustic wavelength, D is the plate thickness, and N is the wave mode number. Resonators are generally operated using the fundamental (N=1) wave mode such that the thickness of the device is equal to half acoustic wavelength. Piezoelectric quartz crystals are traditionally used as electrical frequency filters or as the frequency determining parameters in an oscillator circuit. They can be used as sensors because any addition, removal or change of material at the surface of a QCM can lead to a variation in the device thickness. This will result in a change of resonant frequency of the device (Fig. 5). Sauerbrey [7] first proposed that the change in frequency (Δf) due to a change in thickness of the quartz plate (Δt) would be:

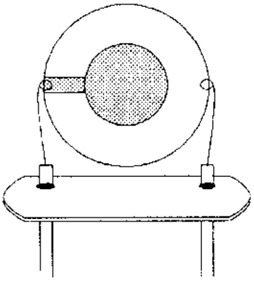

Fig. 4 QCM in standard holder

$$\frac{\Delta f}{f_o}=-\frac{\Delta t}{t} \tag{2}$$

$$t=\frac{M}{A\rho_q} \tag{3}$$

where M=mass of quartz plate, A=surface area, ρ_q=density of quartz and f_o=resonant frequency. Substituting a differential form of Eq. (3) into Eq. (2) gives:

$$\frac{\Delta f}{f_o}=-\frac{M}{tA\rho_q} \tag{4}$$

Sauerbrey assumed that application of foreign material to the face of a QCM would affect the natural frequency of the crystal in the same way as a layer having the same mass. It follows that:

$$\frac{\Delta f}{f_o} = -\frac{\Delta M_s}{tA\rho_q} \qquad (5)$$

where ΔM_s is the mass of any substance deposited on the quartz plate. The resonant frequency, f_o, for an AT-cut quartz crystal vibrating in the thickness shear mode can be expressed as:

$$f_o = \frac{V_q}{2t} \qquad (6)$$

where V_q=velocity of propagation of transverse wave in the plane of the crystal. Substituting [6] into [5] and rearranging gives:

$$\Delta f = -\frac{2f_o^2}{V_q\rho_q}\frac{\Delta M_s}{A} = -C\frac{\Delta M_s}{A} \qquad (7)$$

where C is a constant for a particular quartz crystal. Thus, for example, an AT-cut quartz (ρ_q=2.65 g cm^{-3}, V_q=334 000 cm s^{-1}) crystal with f_o=10 MHz possesses crystal constant C=225963168 Hz g^{-1} cm^2. A 1 Hz shift corresponds to 4.4 ng cm^{-2}. The Sauerbrey equation assumes that the change in resonance due to the uniform depositions of a foreign mass is caused solely by a change to the total thickness of the quartz crystal and the crystal operating in a vacuum.

The Sauerbrey equation is only valid for a thin layer of added mass. More rigorous models have been developed [8–13]. This work has shown that if the added mass is elastic then the following expression is valid for mass loadings as great as 60% of the resonator mass:

$$\frac{\rho_s t_s}{\rho_q t_q} = -\frac{Z_s f_o}{Z_q \pi f}\arctan\left[\left(\frac{Z_q}{Z_s}\right)\tan\left(\frac{\pi f}{f_o}\right)\right] \qquad (8)$$

where Z is the acoustic impedance, ρ is the density and t is thickness. The subscripts s and q represent the added layer and the quartz substrate respectively. If acoustic impedances are not known, then the impedance ratio can be determined by making additional observations at overtone frequencies [13].

Surface acoustic wave devices

Lord Rayleigh first described the phenomenon of waves which occur on the surface of solids [14]. White and Voltmer [15] developed the interdigital transducer (IDT) which allowed the generation of surface waves in piezoelectric

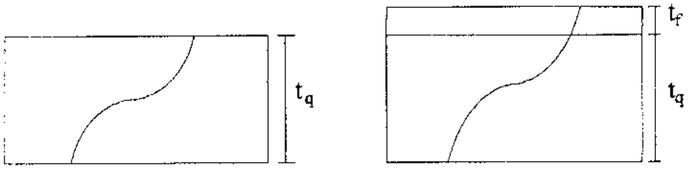

Fig. 5 Addition of thin film on QCM

solids [16–18]. Metal electrodes are deposited on the surface of a piezoelectric solid in the form of thin overlapping fingers (Fig. 6). Alternating fingers are connected to two different bus connection bars. When an alternating voltage is applied across the two bus connectors, oscillating electrical fields are induced between each finger pair. The electrical fields created by the IDT induce particle displacement within the solid. The wave travels along the substrate surface and is then detected with a second IDT through the reverse mechanism. This configuration is known as a delay line because an electrical signal supplied to the input transducer travels 5 times more slowly to the output transducer as an acoustic wave than it would as an electromagnetic signal. The particle displacement of the Rayleigh surface wave has both surface normal and surface parallel components. The combination of these components leads to surface particles moving in an elliptical path. Rayleigh waves have most of their energy localised within one acoustic wavelength of the surface. The wavelength is equal to the transducer periodicity, P, which is the center-to-center distance between two consecutive fingers of one comb of the IDT. The frequency of a SAW device is given by:

$$F = \frac{V}{P} \tag{9}$$

where V is the wave velocity. Typical SAW frequencies are 30–300 MHz. The substrate material used for SAW devices is normally either ST-cut quartz or YZ-$LiNbO_3$. ST-cut quartz has zero temperature coefficient at room temperature. YZ-$LiNbO_3$ has a high piezoelectric coefficient. Silicon can also be used as substrate but as this is not a piezoelectric material, a layer of ZnO or CdS has to be applied. The delay-line need not be piezoelectric. Most SAW sensors (SAWs) employ a dual arrangement of sensor and reference delay lines on one substrate.

In a typical oscillator circuit the device is placed in a feedback loop of an RF amplifier (Fig. 6). The gain of the amplifier must exceed the insertion losses in order for it to continue oscillation. Oscillation will take place at any frequency where the round-trip phase delay is a multiple of 2π. Fractional changes in wave velocity lead to equivalent changes in frequency:

$$\frac{\Delta f}{f} = \frac{\Delta V}{V} \tag{10}$$

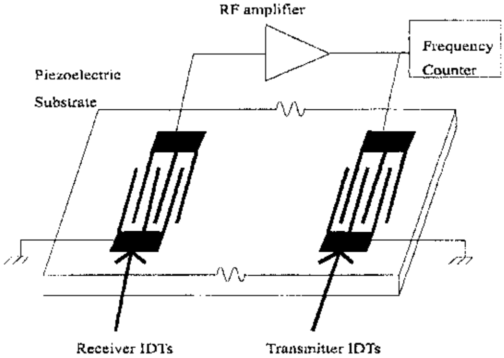

Fig. 6 Delay line SAW sensor

A frequency counter can thus be used as a precise indirect measurement of wave velocity. Analytical information is gained by monitoring the interaction of sample with acoustic wave. In surface acoustic wave sensors (SAWs) if the chemical interaction does not alter the mechanical properties of the film the frequency change is due solely to the added mass [19]:

$$\Delta f = (k_1 + k_2)f_0^2 t_f\rho \qquad (11)$$

where k_1 and k_2 are material constants of the SAW substrate, t_f is the film thickness and ρ is the density and the film mass per unit area is given by $t_f\rho$. Since the resonant frequency of SAW devices is much higher than QCM devices we can see from Eq. (11) that SAW devices will have higher predicted sensitivities. The velocity and amplitude of a Rayleigh wave can be measured by a vector voltmeter. Amplitude measurements provide information about the attenuation of the Rayleigh wave by the medium contacting the surface. This information is useful in determining the properties of thin metal films and can help to identify when velocity changes are not solely due to mass loading. Measurements by vector voltmeters are less sensitive than frequency measurement and are therefore not used for determination of chemical species at low concentrations.

Mass sensing

A number of reviews have described the application of acoustic wave sensors to mass and chemical measurement applications [20–34].The most successful application of QCM sensors has been in the measurement of the deposition of thin metal films in vacuum systems [35]. The measured frequency shift is proportional to the mass of the film. If the film density and acoustic impedance are known, then the film thickness can be obtained. The method is accurate providing the film is thin, stiff and adheres well to the surface. QCM devices have been applied to the detection and quantification of aerosols and suspended particles. Chuan [36] measured the mass of airborne aluminium oxide with a 10 MHz QCM coated with an adhesive layer. The device was reported to yield particulate mass concentrations down to 1 $\mu g\ m^{-3}$. QCMs have been used in conjunction with inertial impactors [37] as well as electrostatic precipitators [38]. SAW resonators have been used to improve the sensitivity of these devices to very small particulates [39].

Acoustic wave microsensors can be used for the measurement of the surface adsorption of vapour molecules at submonolayer coverages. This has been exploited to monitor self-assembly processes and the characterisation of thin films. Self-assembled films range in thickness from one to tens of monolayers. They show promise in a number of fields including catalysts, chemical sensors, lubricants, optical and electronic devices and biological membranes. Crooks *et al.* [40] have used SAW devices to monitor in real-time the self-assembly of *n*-alkylthiol molecules onto Au. It was found that short-chain thiols rapidly form a single monolayer, while long-chain thiols can form structures between one and four monolayers thick. In a separate study, Crooks *et al.* [41] studied the interaction between three different acid-terminated self-assembled monolayer (SAMs) surfaces with three basic vapour phase molecules. The extent of binding is dependent on the acidic and basic properties of the SAMs and the vapour-phase bases. The same group have shown that for an organomercaptan SAM SAW chemical sensor, the variation in response is due to differences in molecular packing and in the ordering of the end groups of the monolayer film [42]. Kurth and Bein [43] used a QCM to show that monomolecular layers of aminopropyltriethoxysilane may be formed on oxidised aluminium substrate and subsequently react with chlorodimethyl silane.

SAW devices have been used for the characterisation of thin films using nitrogen adsorption isotherms, in which the extent of adsorption is measured as a function of nitrogen partial pressure [44]. The adsorption data can be used to determine surface areas by using the BET analysis or to calculate a pore size distribution for the film. The SAW method was found to be 10^4 more sensitive than conventional methods and also avoids errors made in estimating thin-film surface areas from bulk sample measurements. Pfeifer [45] used a SAW sensor to measure the heat of adsorption for H_2O and HCl adsorbing on a Stober sol-gel film as well as determination of the surface area of the film. Adsorption isotherms measured with the SAW device were compared to the BET adsorption model. The heat of adsorption for the first monolayer of H_2O and HCl was found to be 61.1 and 22.2 $kJ\ mol^{-1}$ respectively. The surface area of the film determined using SAWs was found to be a factor of two less than that calculated by SEM images and analysis of particle sizes.

The QCM has been used to study adsorption from the gas phase onto a gold surface. Measurements are made by mixing the substance being studied with a large excess of an inert gas [46]. The total pressure is maintained constant, while the partial pressure of the substance being studied is varied. In a comparison between benzene and pyridine, the study showed that the former is adsorbed flat on the surface, while the latter is attached in an upright position through the nitrogen atom.

Alder *et al.* carried out an in-depth study of the development of humidity correction algorithm for acoustic-wave microsensors [47–51]. The algorithm for correction of sensor responses to a humid challenge gas containing test analyte was based on the fact that water and analyte yield Langmuir isotherms on the coated acoustic wave microsensors.

Acoustic wave gas sensing

Acoustic wave gas sensors employ a chemical layer to collect the analyte gas from the sample stream to the device surface. King first reported the use of QCMs for gas analysis [52, 53]. Wohltjen and Dessy first reported the use of SAW devices for gas analysis [55–56]. Polymer-coated devices have been widely used for gas analysis. The equilibrium distribution of vapour between the gas phase and the sorbent phase is characterized by the partition coefficient, K:

$$K=\frac{C_s}{C_v} \tag{12}$$

where C_s is the concentration of the vapour in the sorbent phase and C_v is the concentration of the vapour in the gas phase. The higher the K value, the greater the amount of vapour collected at the sensor's surface for a given vapour-phase concentration and hence greater the sensitivity of the sensor. Increasing coating thickness also increases the amount of vapour collected at the surface. Too thick a coating leads to the device being overloaded and ceasing to operate [2].

In polymer-coated SAW sensors, the sensor response is the sum of mass effects and modulus changes of the polymer. The latter which arises from polymer swelling due to vapour sorption is the dominant effect. Associated with a surface acoustic wave is an electric wave which travels in the film adjacent to the device surface. If the film has sheet conductivity within a certain range and the SAW device substrate has a high enough electromechanical coupling constant (lithium niobate is ideal), then acoustoelectric interaction is observed between the SAWs and film. Acoustoelectric interaction can lead to changes in the acoustic wave velocity, altering the oscillation frequency of the circuit. Ricco *et al.* [57] have studied the effect of nitrogen dioxide chemisorption on a film of lead phthalocyanine. Chemisorption of nitrogen dioxide leads to an increase in the conductivity of the lead phthalocyanine film. The resulting frequency response is much greater than that due to mass changes alone. The relative contribution of mass loading and conductivity changes on the response of a lithium niobate dual delay line was investigated, by coating one delay line with a layer of chromium followed by coating of both delay lines with films of lead phthalocyanine. Chromium has a high sheet conductivity, thus any further changes in the sheet conductivity of lead phthalocyanine will not affect the resonant frequency. The sensor was determined to be one thousand times more sensitive than an identical SAW sensor functioning via mass loading alone.

Gas sensors operate by binding molecules to the device surface through one of several mechanisms such as absorption, adsorption, chemisorption and complexation chemistry. In the case of adsorption and absorption, the binding strength of the analyte with the chemical coating is weak and thus selectivity is poor but reversibility is high. In the case of chemisorption, very strong interactions occur at the surface of the chemical interface. Since the binding energies are high, the selectivity will be high but reversibility will be poor. If the surface bound material cannot be removed, the detection device becomes a dosimeter. In a less extreme case, the removal of surface bound molecules may require relatively long times or extreme changes in the physical or chemical conditions at the surface. Complexation mechanisms are useful since they have intermediate binding strengths. Complexation mechanisms which have been employed include coordination to metal ions, Lewis acid/Lewis base interactions and charge-transfer interactions [25, 26, 28, 58]. A special case of complexation involves the use of cage or inclusion compounds [59]. Abraham *et al.* report that in a cavitand-coated SAW the selectivity to a vapour is not due to the three-dimensional structure but is governed by general dispersion interactions [60].

In recent years, there has been considerable interest in the use of an array of sensors with each sensor having only a limited selectivity to the measurand and consequently good reversibility. Selectivity to the measurand is achieved through the use of pattern recognition techniques. This strategy is attractive since the system has potential for high selectivity and reversibility. Sensor arrays and pattern recognition can be used in multicomponent analysis [61, 62]. Pattern recognition methods classify different objects (components in mixture) according to the similarities in sensor array pattern. A variety of pattern recognition methods can be used including multiple linear regression, principal component regression, rank annihilation factor analysis, neural networks and fuzzy logic [63, 64]. Abraham et al. [65] have described the solubility interactions relevant to the sorption of non-ionic analytes by sensor materials containing non-ionic organic functional groups. Selectivity to a particular analyte can be increased by maximizing a particular solubility property and minimising all others. For sensor array development, it is suggested that coatings that maximize dispersion interactions, polarizability dipolarity, basicity, basicity and dipolarity, and acidity should all be employed in a sensor array.

Another strategy for increasing the selectivity of a detection system without compromising its reversibility involves use of a sampling device prior to the detector. Kindlund *et al.* [66] have used a teflon-coated tubing prior to the QCM detector to separate water from hydrocarbons (water was retained longer than the hydrocarbons on the tubing). A preconcentration stage prior to detection was also used in this work to determine halogenated hydrocarbons with a silicone oil-coated QCM. Grate *et al.* [67] used a Tenax tube with a SAW sensor array for the determination of DMMP. Thermal desorption of the Tenax tube resulted in separate water and DMMP pulses; water is less well held on the Tenax. Alder *et al.* [68] have used a tungstic acid-coated denuder tube prior to a pyridoxine hydrochloride/antarox CO-880 coated QCM for the determination of low levels of ammonia. The denuder tube affects gas-particle separation; particles with their relatively low diffusion coefficient pass straight through while the gaseous analyte with its high diffusion coefficient is sorbed onto the walls of the tube. The ammonia is thermally desorbed in reference air to the QCM detector. Gas-particle separation is important since their interaction can result in artifacts leading to an under- or over-estimation of the analyte. In the atmospheric determination of ammonia, decomposition of ammonium salts on filters prior to a detection system can lead to release of ammonia and thus an overestimation of ammonia gas concentration. Denuder tubes have the additional advantage that they introduce an extra stage of selectivity and can allow pre-concentration of the analyte.

Liquid phase sensing

Kanazawa and Gordon [69] and Bruckenstein and Shay [70] showed that a QCM would oscillate in liquids and the frequency shift is of the form:

$$\Delta f = -k f_0^{3/2} (\mu\rho)^{1/2} \tag{13}$$

where μ is the liquid viscosity, ρ is the liquid density and k is a constant. The form of this equation agrees with experimental data [71] but deviations have been observed due to non-ideal behaviour. Frequency shifts greater than those predicted on the basis of liquid density and viscosity have been ascribed to surface roughness of the QCM, interfacial effects and viscoelastic changes of the films coated on the QCM. Liquid-phase operation of acoustic wave microsensors is predicted if wave motion produces surface normal particle displacement and the wave propagation velocity is greater than the velocity of sound in liquid; this is the case in SAW devices [1, 2]. With QCMs, viscous coupling between the surface and the liquid results in a damped shear wave that propagates into the liquid with a characteristic decay length. The decay length for a 5-MHz QCM is ~0.25 μm in water. The entrained liquid layer decreases the resonant frequency and damps the QCM resonance.

It has been shown that the effects of viscoelastic layers and liquids can be modelled by observing the relationship between complex electrical impedance and frequency of QCMs. It has, therefore, been possible to discriminate responses due to surface mass changes and from responses to changes in liquid properties by using a network analyzer [72]. Hayward and Chu [73] described an inexpensive system for simultaneous measurement of mass and viscosity in under-liquid QCM sensing. The system employs an automatic gain control (AGC) oscillator. The AGC voltage is affected only by the liquid medium so that a viscosity or density correction can be applied oscillator. Further information about non-rigid overlayers can be obtained by determining the damping of the QCM oscillation which is known as the dissipation factor and is the inverse of the Q factor. Rodahl *et al.* [74] have described systems for simulataneous measurement of resonant frequency and dissipation factor. Clavo *et al.* [75] have described a system for deconvolution of rigid mass and viscous resistance by measurement of input and output ac voltages.

In recent years a new technique known as electrochemical quartz crystal microbalance (EQCM) has been developed. In this technique, the exciting electrode of a QCM is under potential control and made part of an electrochemical cell; the technique can be used to study electrochemically driven processes. EQCM has been used to monitor the UPD process in-situ while metal deposition is taking place [76]; it has also been used to study mass transport that accompanies redox processes in thin films on electrodes [77]. EQCM applications have been reviewed elsewhere [5, 78, 79].

QCM based biosensors are developed by immobilising a bioactive component to the device surface [6, 80, 81]. The ligand-receptor binding event can be monitored by observing the frequency change of the QCM. The bioactive components are generally either the catalytic or the affinity binding types. The catalytic type are generally enzymes or biological organisms. The affinity binding type includes bioactive components such as antibodies, lectins, receptor proteins and nucleic acids. It is possible to immobilise an enzyme to the surface of a device and to directly monitor the binding of the enzymes substrate; such binding is more reversible than antigen-antibody binding. Antibodies are selective binding agents to antigens and are used in a wide variety of immunoassay. It is difficult to produce antibodies for low molecular weight antigens. Antibodies have been used for the assay of drugs, microorganisms, nucleic acids, hormones and other proteins. Other selective binding agents include lectins which are proteins able to bind to carbohydrates. Single-stranded DNA can be immobilised in order to obtain selective binding to complementary strands of DNA or RNA. DNA probes are particularly applicable to the detection of viruses.

Methods used in the immobilisation of a bioactive component to the device surface can be classified into the following categories: physical adsorption, covalent bonding and polymer entrapment. At present, the most widely-used method is covalent bonding. Quartz may be classified as oxides; the sensor surface therefore appears as an array of metal oxides. The surface may be hydrated and therefore hydroxide groups and water molecules may also be present on the surface. The sensor surface can be pre-treated to alter its characteristics, e.g. a sensor surface pre-treated with dimethyldichlorosilane will lead to a hydrophobic surface while a surface that is pretreated with aminopropyltrimethoxysilane will be hydrophilic. Physical adsorption of proteins and other large molecules takes place through a combination of Van der Waals, ionic, hydrophobic and hydrogen bond forces. Two major disadvantages exist for physical adsorption. Firstly, the bioactive component is randomly oriented on the sensor surface. This could lead to changes in protein conformation, thus altering the properties of the bioactive component. The second disadvantage is that in physical adsorption the binding is weak, leading to the bioactive component being washed off the sensor surface. In covalent bonding, the bioactive component is more strongly held to the sensor surface and is therefore less likely to be washed away. By making appropriate choice of immobilisation chemistry it is also possible to control the orientation of the bioactive component to the sensor. The major disadvantage of polymer entrapment is that often thick films are produced as compared with covalent bonding and adsorption. Thicker films would adversely effect the kinetics of mass transfer of analyte to and away from the sensor surface leading to reduced sensor response times.

The first QCM biosensor was reported by Shons *et al.* [82]. In this work, QCMs with gold electrodes were dipped into various protein solutions. The protein-coated QCMs were then allowed to dry in an environmental chamber with controlled temperature and humidity and the resonance frequency was measured. The protein-coated QCMs were then exposed to solutions containing antibodies to the proteins of the intial coating and also to other non-antibody proteins. The QCMs were allowed to dry after the second exposure to solution and the resonance frequency was measured. The difference frequency was used to obtain qualitative and quantitative assay of antibody activity. This approach of measurement QCM response only in the dry phase has come to be known as a dip and dry measurement. The dip and dry approach has also been used in the competitive immunoassay of antigens [83]. The QCM was first coated with antigen and then exposed to a solution containing an unkown amount of antigen and to which a known amount of antibody to the antigen was added. The antibody was bound to the antigen in the bulk and also to the antigen on the surface of the QCM. A greater amount of antigen in the bulk solution leads to a smaller amount of antibody binding to the antigen on the surface of the QCM. This allows measurement of the amount of antigen in the bulk solution to be determined. Antigen quantities as low as 10^{-11} M could be detected.

QCMs have also been used for determination of the amount and subclass of antibodies present in solution [84]. An antigen to a given antibody is coated on the QCM surface and then the QCM is exposed to a solution of antibody. The resulting frequency change is used to quantify the amount of antibody. The QCM now has an antigen to which the antibody is bound. The QCM is then exposed to solutions containing antibodies which are specific to individual subclasses of antibody. Additional binding of the second antibody indicates the subclass of the first antibody. Reduction in non-specific adsorption of sample matrix proteins onto the QCM was achieved by using a variation of the previous scheme [85]. An antibody was detected with an antigen-coated sensor; the resulting frequency change was not used for quantification since other proteins present may have also adsorbed. Instead, a second reagent capable of specifically binding to the first antibody is added and resulting frequency change is used to quantify the amount of the first antibody present.

Guilbault *et al.* [86] has reported the use of QCM coated with antibodies to parathion for the determination of parathion in the vapour phase. Cross-reactivity to other pesticides such as malathion were observed. Thompson *et al.* [87] have disputed that antibody-coated QCMs can bind with immunologically based specificity in the vapour phase. Bare gold electrode QCMs have been shown to respond to pesticide compounds having sulfur atoms. Ebersole and Ward have indirectly monitored antigen/antibody interaction [88]. Through a series of steps, a precipitate is formed which is deposited on the sensor surface leading to a much larger frequency change than the original antigen/antibody interaction. A glucose biosensor has been reported which employs a QCM coated with the enzyme hexokinase. Reversibility is maintained by preventing the enzyme catalyzed reaction from going to completion, this was done by omitting necessary cofactors [89]. Changes in the viscoelastic properties of the liquid adjacent to a sensor surface have been used as a basis of analyte detection. Limulus amebocyte lystate (LAL) will be gelled by exposure to endotoxin and this can be monitored by observing frequency changes [90].

Conclusions

Acoustic wave mass sensors are very promising for thin film characterisation, gas and under-liquid sensing. The number of applications to which they are applied in the future will increase. Since acoustic waves can be generated by a variety of methods future research will involve the development of new device structures, which are less affected by the environment, have higher mass sensitivities and are smaller. Mass sensitivities can be increased by the use of amplification strategies and improved methods of coating immobilisation. The use of acoustic wave sensors in sensor arrays with novel pattern recognition algorithms for gas analysis is exciting. Acoustic wave sensor arrays have the relative advantage over conducting polymer-based sensor arrays in that they are more applicable to relatively non-volatile compounds. The use of QCMs in liquids greatly extends their applications. It should, however, be remembered that with viscous mass layers, as with large biomolecules, the acoustic wave will be attenuated while propagating through these layer. It is likely that we will see further developments in the theory and measurement techniques for sensing in liquids.

References

1 J. W. Grate, S. J. Martin and M. W. Richard, Anal. Chem., 55 (1993) A940.
2 J. W. Grate, S. J. Martin and M. W. Richard, Anal. Chem., 55 (1993) A987.
3 J. Curie and P. Curie, Bull. Soc. Min. Paris, 3 (1880) 90.
4 G. Lippmann, An. Chim. Phys. Ser. 5, 24 (1881) 145.

5 D. A. Buttry and M. D. Ward, Chem. Rev., 92 (1992) 1355.
6 G. J. Bastiaans, Chemical Sensor Technology, Vol. 4 (Ed. S. Yamauchi), Elsevier, Amsterdam 1992, p. 181.
7 G. Z. Sauerbrey, Z. Phys., 155 (1959) 206.
8 C. D. Stockbridge, Vacuum Microbalance Techniques, Vol. 5 (Ed. K. Behrndt), Plenum Press, New York 1966, p. 193.
9 J. G. Miller and D. I. Bolef, J. Appl. Phys., 39 (1968) 4589.
10 C. S. Lu and O. Lewis, J. Appl. Phys., 43 (1972) 4385.
11 C. S. Lu, J. Vac. Sci. Tech., 12 (1975) 578.
12 E. Sollner, A. Benes, A. Biedermann and D. Hammer, Vacuum, 27 (1977) 367.
13 E. Benes, J. Appl. Phys., 56 (1984) 608.
14 Lord Rayleigh, London Math. Soc. Proc., 17 (1887) 4.
15 R. M. White and F. W. Voltmer, Appl. Phys. Lett., 7 (1965) 314.
16 J. D. Maines, E. G. S. Paige, A. F. Saunders and A. S. Young, Electronics Lett., 5 (1969) 678.
17 D. P. Morgan, Ultrasonics, 11 (1973) 121.
18 E. Dieulesaint and D. Royer, Elastic Waves in Solids (Appliations to Signal Processing), Wiley, Chichester 1980, Ch. 7.
19 B. A. Auld, Acoustic Fields and Waves in Solids, Vol., 2, Wiley-Interscience, New York 1973, p. 271.
20 J. Hlavay and G. G. Guilbault, Anal. Chem., 49 (1977) 1890.
21 L. M. Webber, J. Hlavay and G. G. Guilbault, Microchimica Acta, (1978) 351.
22 J. F. Alder and J. J. McCallum, Analyst, 108 (1983) 1169.
23 G. G. Guilbault, Methods and Phenomena, Vol. 7 (Eds. C. Lu and A. W. Czanderna), Elsevier, New York, 1984 p. 251.
24 H. Wholtjen, Sens. Actuators, 5 (1984) 307.
25 M. S. Niewenhuizen and A. W. Barendsz, Sens. Actuators, 11 (1987) 45.
26 G. G. Guilbault and J. M. Jordon, CRC Critical Reviews Anal. Chem., 19 (1988) 1.
27 G. J. Bastiaans, Chemical Sensors (Ed. T. E. Edmond), Chapman and Hall, New York 1988, p. 295.
28 M. S. Niewenhuizen and A. Venema, Sensor Materials, 5 (1989) 261.
29 A. D'Amico and E. Verona, Sens. Actuators, 17 (1989) 55.
30 C. G. Fox and J. F. Alder, Analyst, 114 (1989) 997.
31 J. Janata, Principles of Chemical Sensors, Plenum Press, New York 1989, p. 55.
32 M. S. Nieuwenhuizen and A. Venema, Sensors: A Comprehensive Survey, Vol. 2 Part 1 (Eds. W. Gopel, J. Hesse and J. N. Zemel), VCH, Weinheim 1991, p. 648.
33 B. R. Eggins, Biosensors; An Introduction, Wiley, Chichester 1996, p. 121.
34 M. J. Hepher and D. Reilly, Sensor Systems for Environmental Monitoring, Chapman and Hall, London 1997, p. 179.
35 C. S. Lu and A. W. Czanderna, Applications of Piezoelectric Quartz Crystal Microbalance, Elsevier, New York 1984.
36 R. L. Chuan, J. Aerosol Sci., 1 (1970) 111.
37 T. E. Carpenter and D. L. Brenchley, Am. Ind. Hyg. Assoc. J., 33 (1973) 503.
38 J. G. Olin and G. J. Sem, Atmos. Environ., 5 (1971) 653.
39 W. D. Bowers, R. Duong and R. L. Chaun, Rev. Sci. Instrum., 62 (1991) 1624.
40 R. C. Thomas, L. Sun, R. M. Crooks and A. J. Ricco, Langmuir, 7 (1991) 620.
41 H. C. Yang, D. L. Dermody, C. J. Xu, A. J. Ricco and R. M. Crooks, Langmuir, 12 (1996) 726.
42 R. C. Thomas, H. C. Yang, C. R. Dirubio, A. J. Ricco and R. M. Crooks, Langmuir, 12 (1996) 2239.
43 D. G. Kurth and T. Bein, Angew. Chem. Int. Ed. Engl., 31 (1992) 336.
44 A. J. Ricco, G. C. Frye and S. J. Martin, Langmuir, 5 (1989) 273.
45 K. B. Pfeifer, Langmuir, 11 (1995) 4793.
46 V. Tsionsky and E. Gileadi, Langmuir, 10 (1994) 2830.
47 C. G. Fox and J. F. Alder, Anal. Chem. Acta, 248 (1991) 337.

48 J. T. Wood and J. F. Alder, Talanta, (1992) 39, 11, 1505.
49 F. Benmakroha and J. F. Alder, Anal. Chim. Acta, 302 (1995) 55.
50 F. Benmakroha and J. F. Alder, Anal. Chim. Acta, 317 (1995) 281.
51 F. Benmakroha and J. F. Alder, Anal. Chim. Acta, 343 (1997) 215.
52 W. H. King, Anal. Chem., 36 (1964) 1735.
53 W. H. King, US Patent 3 164004, 1965.
54 H. Wohltjen and R. Dessy, Anal. Chem., 51 (1979) 1458.
55 H. Wohltjen and R. Dessy, Anal. Chem., 51 (1979) 1465.
56 H. Wohltjen and R. Dessy, Anal. Chem., 51 (1979) 1470.
57 A. J. Ricco, S. J. Martin and T. E. Zipperian, Sens. Actuators, 8 (1985) 319.
58 A.W. Snow and W. R. Barger, Phthalocyanines Properties and Applications (eds. B. P. Lever and C. C. Leznoff), VCH, New York 1989, Ch. 5, p. 341.
59 C. S. Lai, G. J. Moody, J. D. R. Thomas, D. C. Mulligan, J. F. Stoddart and R. Zarzycki, J. Chem. Soc., Perkin Trans., 2 (1988) 319.
60 J. W. Grate, S. J. Patrash, M. H. Abraham and C. M. Du, Anal. Chem., 68 (1996) 913.
61 D. S. Ballantine, S. L. Rose, J. W. Grate and H. Wohltjen, Anal. Chem., 58 (1986) 3058.
62 W. P. Carey and B. R. Kowalski, Anal. Chem., 58 (1986) 3077.
63 R. Muller, Sensors: A Comprehensive Survey, Vol. 1 (Eds. W. Gopel, J., Hesse J. N. Zemel), VCH, Weinheim (1989), Ch. 11, 314.
64 U. Weimar, S. Vaihinger, I. C. D. Schierbaum and W. Gopel, Chemical Sensor Technology, Vol. 3 (Ed. N. Yamazoe), Elsevier, Amsterdam 1991, p. 51.
65 J. W. Grate and M. H. Abraham, Sens. Actuators B, 3 (1991) 85.
66 A. Kindlund, H. Sundgren and I. Lundstrom, Sens. Actuators, 6 (1984) 1.
67 J. W. Grate, S. L. Rose-Pehrsson, D. L. Venezky, M. Klusty and H. Wohltjen, Anal. Chem., 65 (1993) 1868.
68 Z. Ali, C. L. P. Thomas, J. F. Alder and G. B. Marshall, Analyst, 117 (1992) 899.
69 K. K. Kanazawa and J. G. Gordon, Anal. Chem., 57 (1985) 1770.
70 S. Bruckenstein and M. Shay, Electrochim. Acta, 30 (1985) 1295.
71 T. Nomura and M. Okuhara, Anal. Chim. Acta, 142 (1982) 281.
72 A. L. Kipling and M. Thompson, Anal. Chem., 62 (1990) 1514.
73 G. L. Hayward and G. Z. Chu, Anal. Chim. Acta, 288 (1994) 179.
74 M. Rodahl and B. Kasemo, Sens. Actuators B, 37 (1996) 111.
75 E. J. Calvo, C. Danilowicz and R. Ethcenique, J. Chem. Soc., Faraday, Trans., 91 (1995) 4083.
76 O. Melroy, K. K. Kanazawa, J. G. Gordon and D. Buttry, Langmuir, 2 (1986) 697.
77 S. Bruckenstein, C. P. Wilde, M. Shay, A. R. Hillman and D. Loveday, J. Electroanal. Chem., 258 (1989) 457.
78 R. Schumacher, Angew, Chem. Int. Ed. Eng., 29 (1990) 329.
79 S. Bruckenstein and A. R. Hillman, Handbook of Surface Imaging and Visualization (Ed. A. T. Hubbard) CRC Press, Boca Raton, 1995 p. 101.
80 A. A. Suleiman and G. G. Guilbault, Analyst, 119 (1994) 2279.
81 M. Minunnu, M. Mascini, G. G. Guilbault and B. Hock, Anal. Letters, 28 (1995) 749.
82 A. Shons, F. Dorman and J. Najarian, J. Biomed. Mater. Res., 6 (1972) 565.
83 R. J. Olivera and S. F. Silver, US Patent 4, 242, 096 (1980).
84 T. K. Rice, US Patent 4, 236, 893 (1980).
85 T. K. Rice, US Patent 4, 314, 821 (1982).
86 J. Ngeb-Ngwainbi, P. H. Foley, S. S. Kuan and G. G. Guilbault, J. Amer. Chem. Soc., 108 (1986) 5444.
87 L. Rajakovic, V. Ghaemmaghami and M. Thompson, Anal. Chem. Acta, 217 (1989) 111.
88 R. C. Ebersole and M. D. Ward, J. Amer. Chem. Soc., 110 (1988) 8623.
89 S. J. Lasky and D. A. Buttry, Chemical Sensors and Microinstrumentation (Eds. R. Murray, R. E. Dessy, W. R. Heineman, J. Janata and W R Seitz) Amer. Chem. Soc., Washington, 1989, p. 237.
90 H. Muramatsu, E. Tamiya, M. Suzuki and I. Karube, Anal. Chim. Acta, 217 (1989) 321.